

CFD modelling and the development of the diffuser augmented wind turbine

D. G. Phillips[†], P. J. Richards[‡] and R. G. J. Flay^{‡†}

Department of Mechanical Engineering, The University of Auckland, Private Bag 92019, Auckland, New Zealand

Abstract. Research being undertaken at the University of Auckland has enabled Vortec Energy to improve the performance of the Vortec 7 Diffuser Augmented Wind Turbine. Computational Fluid Dynamic (CFD) modelling of the Vortec 7 was used to ascertain the effectiveness of geometric modifications to the Vortec 7. The CFD work was then developed to look at new geometries, and refinement of these led to greater power augmentation for a given diffuser exit area ratio. Both full scale analysis of the Vortec 7 and a wind tunnel investigation of the development design have been used for comparison with the CFD model.

Key words: DAWT; diffuser augmented wind turbine; CFD; computational fluid dynamic modelling; PHOENICS; low-Reynolds number; k - ϵ turbulence model; wind tunnel; Vortec Energy.

1. Introduction

A diffuser augmented wind turbine (DAWT) has a duct which surrounds the wind turbine blades and increases in cross-sectional area in the streamwise direction. The resulting sub-atmospheric pressure within the diffuser draws more air through the blade plane, and more power can be generated compared to a “bare turbine” of the same rotor blade diameter.

Several researchers have examined the benefits and economics of placing a diffuser around a wind turbine. A theoretical study was undertaken by Lilley and Rainbird at Cranfield in 1956. The work identified the benefits of a DAWT. An extensive programme of experimental work performed at the Grumman Aerospace Corporation in the 1970's and early 1980's identified the use of external air jets to prevent separation within the diffuser (Foreman and Gilbert 1983). The high speed jet flows were achieved through a “slotted diffuser” design and re-energised the boundary layer within the diffuser enabling a short length-to-diameter diffuser with a large outlet-to-inlet area ratio to be developed (Foreman *et al.* 1983). This experimental work by Foreman and co-workers led to more economical designs. Their best design was the basis of the Vortec 7, a technology demonstration unit built by Vortec Energy Limited.

However, the economical benefits derived from Foreman's slotted diffuser design were not seen until 1997. It was the use of High Tensile Reinforced Fibrous Ferrocement (HT Ferro) that enabled Vortec Energy to secure the rights to the design and the production of the first full scale DAWT

[†] Ph.D. Student

[‡] Associate Professor

^{‡†} Professor



Fig. 1 The Vortec 7. Flow is from left to right. The curved boundary layer slot is seen near the outlet on the right

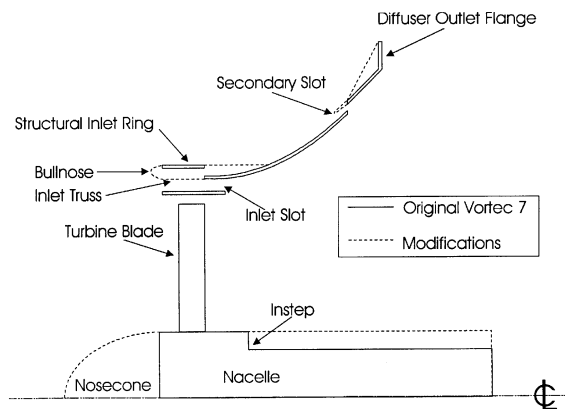


Fig. 2 Axi-symmetric cross section of the Vortec 7

(Nash 1997). The Vortec 7 has a rotor blade diameter of 7.3 m and is situated near the Franklin west coast, 120 km south of Auckland, New Zealand. The as-built Vortec 7 is shown in Fig. 1 with the main geometric features shown in Fig. 2.

A CFD model has been developed to test various geometric variations to the Vortec 7 diffuser. It has been used as a cost-effective tool for the improvement of the Vortec 7 performance and for the development of diffuser concepts for a production Vortec with significantly improved performance compared to the Vortec 7. Data from the Vortec 7 have been used for validation of the CFD model together with wind tunnel analysis of a more refined design, referred to as the development diffuser.

2. CFD model of the original Vortec 7

The fully viscous, finite volume code PHOENICS was used for the CFD modelling. An initial

study investigated the effects of the diffuser shape and boundary layer control slots of the as-built Vortec 7 and subsequent modifications. The model is axi-symmetric with specified inlet conditions and reference length making the model dimensionless. A structured multi-block body-fitted grid is used to reproduce the complex geometry of the DAWT. The turbine is modelled as a flow resistance and has a specified thrust coefficient that produces a pressure drop across the blade plane proportional to the local dynamic pressure.

$$C_{t2} = \frac{P_2 - P_3}{0.5\rho V_3^2} = \text{local disc or thrust loading coefficient}$$

where P_2 static pressure immediately upstream of blade plane
 P_3 static pressure immediately downstream of blade plane
 V_3 velocity at the blade plane

This is analogous to the use of a gauze screen in wind tunnel testing (Gilbert *et al.* 1978). The flow is assumed to have no swirl and only the global effect of the blades was modelled. The Vortec 7 has an inlet truss (Fig. 1) for structural reasons and this was modelled by a shear stress acting in both the axial and radial directions over the cells in the inlet boundary layer control slot. The shear stress is scaled by the area ratio of the triangular geometry to the cell area in order to match the CFD model to the physical Vortec 7. The k - ε turbulence model has been used with uniform inlet boundary conditions specified for k and ε . The values of k and ε have been calculated for the hub height and terrain in which a turbine would be situated (Richards and Hoxey 1993). The diffuser surfaces were specified as non-slip boundaries with wall functions used to describe the wall boundary conditions.

It is recognised that the CFD turbine model is a simple one, which ignores the features of flow swirl caused by an operating turbine, and the effect of a gauze screen on damping out turbulence. It is thought that the addition of swirl within the diffuser would have a beneficial effect on performance through a reduction of flow separation along the diffuser wall. Additionally, vorticity shed at the blade tip is anticipated to enhance mixing within the diffuser, particularly in the vicinity of the wall. Although swirl and vorticity in the flow are expected to improve the performance of the diffuser, they will reduce the efficiency of the blades, and so to some extent ignoring them in the CFD model is self compensating. In representing the turbine in the wind tunnel by a gauze screen, additional effects are introduced. Gauze screens tend to damp turbulence (related to their pressure drop coefficient) and this could be expected to alter the boundary layer on the diffuser wall. This is different from the situation with an operating turbine where turbulence with scales less than the distance between consecutive slices of the air by the blades would be expected to pass through the diffuser relatively unscathed. As a result of this difference the CFD model did not include a turbulence sink at the blade plane. Another possible effect associated with gauze screens is flow refraction where it bends if approaching a screen at a direction other than normal to it. This is not thought to be significant in the current situation, since the flow can be expected to be essentially normal to the blade plane and is contained within a closed duct, which would impede refraction. Although it is possible to construct a more complex turbine model, which could include secondary effects associated with either the rotating turbine or the gauze screen, but probably not both, it is uncertain whether such refinements would improve the overall model. The assumptions simplified the computational model whilst retaining the most important features of the flow and allowed the

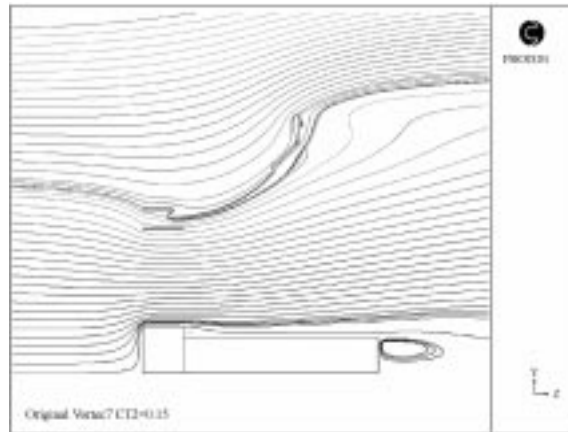


Fig. 3 Streamline plot showing flow reversal through inlet truss for the original Grumman design. Flow separation can be seen on the inner wall of the primary diffuser

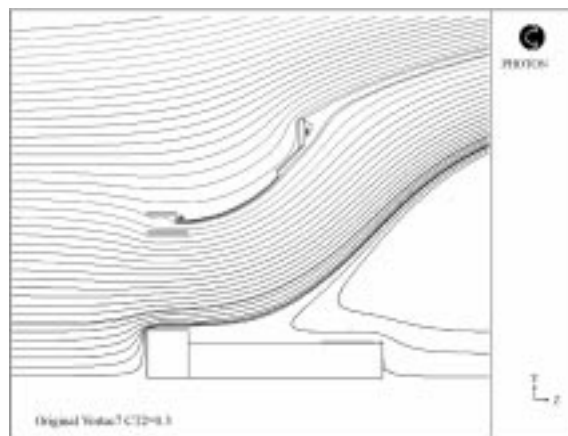


Fig. 4 Streamline plot showing flow separation from the nacelle for a disc loading coefficient of 0.3 on the original Grumman design

CFD modelling to be used for rapid development of diffuser designs.

An initial CFD model of the as-built Vortec 7 geometry was developed for comparison with Vortec 7 site data (Phillips *et al.* 1999). The results obtained were compared with flow visualisation using smoke and spinnaker cloth tufts attached to the walls of the diffuser. At that time there were no data available for quantitative comparison. The CFD model correctly predicted separation downstream of the nacelle and the diffuser outlet flange. Another important observation was the reversal of flow around the structural inlet ring of the Vortec 7, which is shown in Fig. 3. This was also seen during smoke testing of the Vortec 7. It was found that the CFD model also predicted the high velocity speed-up through the inlet slot and the radial variation of flow speed across the blade plane that was observed in preliminary site measurements. The effect of the disc loading was studied and showed that at high disc loading the flow was forced out towards the diffuser and reduced the separated region on the diffuser. This effect was observed with the Vortec 7 by varying the rotational speed of

the turbine. This consequently created a large region of reversed flow around the nacelle. Velocity and directional anemometry sensors located on a boom at the diffuser exit clearly showed the separated region next to the nacelle and the high diffusion angles outside that region. These observations confirmed the streamline plots obtained with the CFD model. Figs. 3 and 4 provide a comparison of the streamlines for the thrust coefficient 0.15 and 0.3 cases respectively. In Fig. 3 flow separation can be seen on the inner wall of the primary diffuser whereas in the higher loading case of Fig. 4 the flow remains attached to the diffuser but separates from the nacelle.

3. Modifications to the Vortec 7 geometry

The power obtained from the original Vortec 7 was lower than predicted by Foreman. It is believed that this is mainly a result of the separation found on the prototype. A CFD study was therefore undertaken to examine various geometric alterations in order to ascertain their effectiveness in reducing the separated flow. Modifications included an elliptical nosecone, a bull-nose fitted to the inlet slot to prevent the flow reversal observed initially, and modifying the secondary inlet slot and diffuser to direct flow tangentially to the diffuser wall. Finally the instep in the nacelle was removed with the addition of foam sections to match the change in geometry from the circular spinner to the pentagon shaped nacelle (Figs. 2 and 5). With the modifications incorporated into the Vortec 7 numerical model a substantial improvement in power was achieved as shown in Fig. 6, where the available air power coefficient is defined by the following equation.

$$C_{P_{air}} = \frac{V_3^3 C_{t2}}{V_\infty^3} = \text{Available air power coefficient}$$

where C_{t2} local disc loading coefficient
 V_∞ ambient velocity well upstream of the diffuser
 V_3 velocity at the blade plane

Although the CFD model predicted that the modified design would have flow attached to both the nacelle and diffuser, intermittent flow separation was still observed on the trailing third of

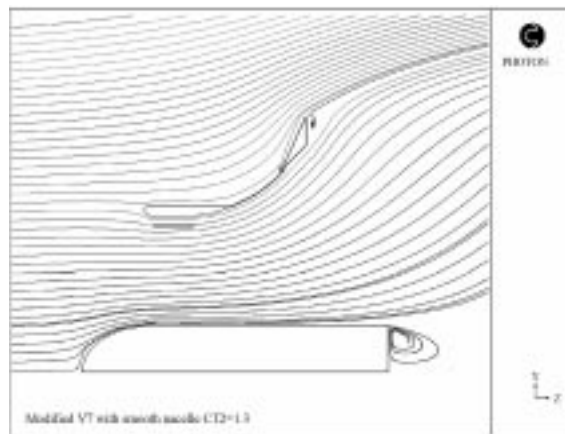


Fig. 5 Streamline plot for the modified Vortec 7

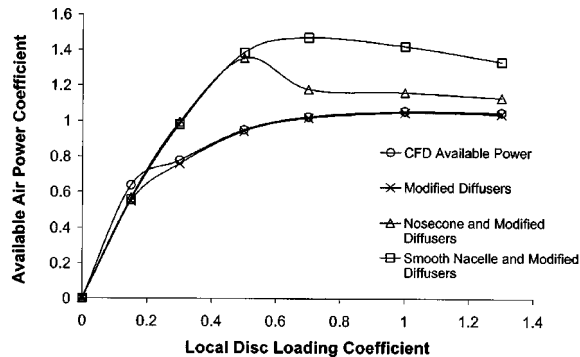


Fig. 6 Comparison of available air power for the Original Vortec 7 and subsequent modifications

the full scale Vortec 7 primary diffuser and along the nacelle. Although an improvement in power was found, it did not match the predictions at Grumman (Foreman and Gilbert 1983, Foreman *et al.* 1983). It was, however, a significant increase compared to a bare turbine of the same blade diameter.

4. Advanced diffuser designs

The CFD model of the Vortec 7 has been the starting point for the development of new diffuser designs. The effect of the inlet slot, diffuser outlet flange, nacelle shape and size have been examined using the existing area ratio and diffuser exit angle as discussed above. However, a step jump in performance was desired and so a new design was developed which introduced controlled contraction of the flow into the blade plane. The primary diffuser was extended upstream and the inner inlet ring removed. The area ratio and diffuser angle were altered for this new geometry and the diffuser exit flange removed. Increases in power coefficient by a factor of approximately two compared with the original were predicted by the CFD. An example of the new geometry is shown in Fig. 7. The new geometry with controlled inlet contraction displayed similar trends to those predicted by a one-dimensional analysis (Phillips *et al.* 1999). Much larger speed-ups at the blade

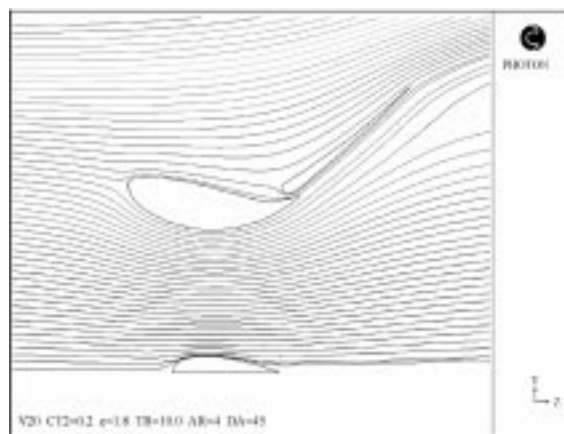


Fig. 7 Streamline plot of the development diffuser

plane were predicted with the optimal power coefficient, of around 1.9, occurring at a local disc loading coefficient between 0.3 and 0.4.

5. Wind tunnel verification

To verify the predictions for the development geometry a series of wind tunnel investigations were conducted. The first series of tests were performed in the 3 by 2 metre closed section wind tunnel at Vipac Engineers and Scientists Limited, Melbourne, Australia. Various wire screen meshes were used to produce a range of pressure drops across the blade plane. The total pressure drop across the mesh, the velocity speed-up, and the base (exit) pressure were measured with pitot-static probes referenced to an upstream pitot-static probe in the free-stream flow. These measurements provided the information required to characterise the DAWT performance and allow comparisons with the CFD predictions. Figs. 8 and 9 show the wind tunnel results for power coefficient, velocity speed-up and base pressure coefficient. These are compared with two CFD predictions. Fig. 8 shows CFD results which ignore the presence of the wind tunnel walls. The CFD results show a less negative base pressure than the wind tunnel. It was suspected that the blockage effect created by the closed wind tunnel test section accelerated the flow around the outside of the diffuser artificially lowering the base pressure and causing this mismatch in results. Further CFD runs were therefore done where

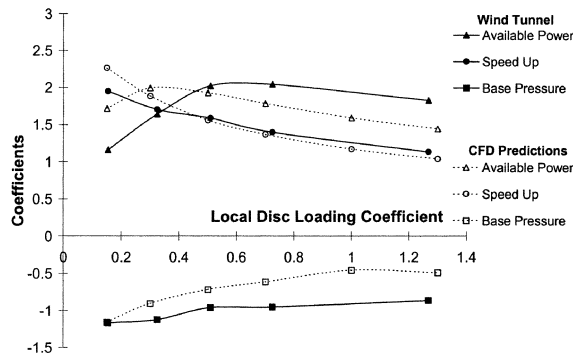


Fig. 8 Comparison of wind tunnel results and CFD predictions with no blockage correction

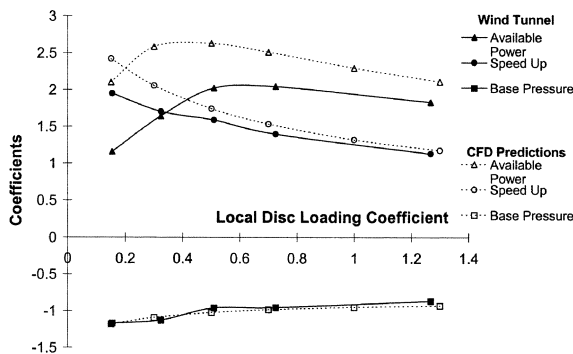


Fig. 9 Comparison of wind tunnel results and CFD predictions incorporating a solid boundary at the wind tunnel hydraulic diameter

the blockage was accounted for in the model with the addition of a solid boundary at the hydraulic diameter of the wind tunnel. Good agreement was then obtained for the base pressure as shown in Fig. 9. It was noted during wind tunnel flow visualisation that several regions of the flow exhibited separation. These were not predicted in the CFD model, probably due to the use of the $k-\varepsilon$ turbulence model together with wall functions on the diffuser surfaces. It is suspected that this is the reason for the over-prediction of the power by the CFD analysis compared to the wind tunnel in Fig. 9.

6. Refinement of the CFD model

The comparison made with the wind tunnel studies indicated that the CFD model required improvement in order to correctly predict the flow patterns and available air power observed during testing. Separation was not predicted in the CFD solutions on the outer surface of the primary diffuser at any disc loading and only to a limited extent within the diffuser. To improve the prediction of separation and agreement with wind tunnel results, refinement of the CFD model to include integration of the flow equations through the viscous sublayer was necessary. PHOENICS version 2.1 utilises a matched multi-block grid which therefore requires the use of a H-type grid around the diffuser geometry. To reduce non-orthogonality, an algebraic mesh with cubic splines defining the block boundaries was developed. In the flow direction care was taken to ensure the grid was aligned to the flow to reduce numerical diffusion. Cell spacing in the normal direction around the diffuser was described by sine and cosine functions with a geometric progression used to expand the mesh out to the domain boundaries. The Lam-Bremhorst low-Reynolds number extension to the $k-\varepsilon$ turbulence model was available in PHOENICS 2.1. This model gives improved prediction of separation in flows with large adverse pressure gradients compared with the standard high-Reynolds number turbulence model. Details of the model and its implementation are available in the PHOENICS On Line Information System (POLIS). As the low-Reynolds number turbulence model does not employ wall functions, the flow field has to be meshed into the laminar sublayer and down to the wall with the first grid point normal to the wall not exceeding $Y^+ = 4.0$. An increase in the computational mesh from around 25000 cells to 37000 cells was required. Due to the use of a structured H-type body-fitted grid, numerical instability meant it was only possible to obtain

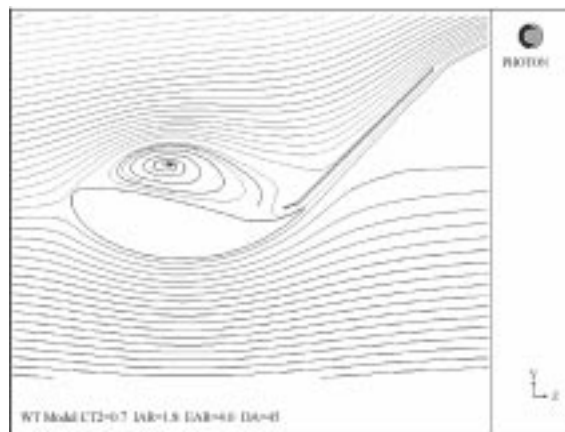


Fig. 10 Streamline plot for the refined development diffuser CFD model

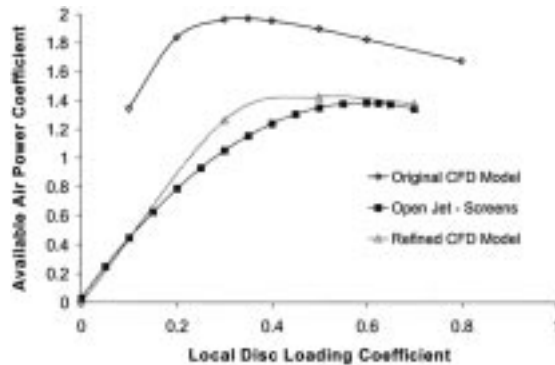


Fig. 11 Available air power comparison for the original CFD model, the refined CFD model and wind tunnel data for the development diffuser

solutions up to a local disc loading coefficient of 0.7. For the solutions obtained a substantial change in both the flow patterns and available air power predicted was achieved which brought the CFD results closer to the wind tunnel observations. Separation was predicted over the outer surface of the primary diffuser as seen in Fig. 10 together with a region of nearly stationary flow adjacent to the inside of the secondary diffuser. Fig. 11 shows the effect of this separation on the prediction of available air power which is dramatically reduced. Fig. 11 also shows wind tunnel test results on the same model as for Figs. 8 and 9, but obtained subsequently in the University of Auckland Twisted Flow Wind Tunnel in its Open Jet 3 m \times 3 m configuration. The results in Fig. 11 are considered to be more reliable than the earlier results due to the reduction in blockage, and the improvement in experimental techniques. This is why these wind tunnel results predict lower air power than Figs. 8 and 9. Agreement between the wind tunnel results and the refined CFD model occurs for disc loading coefficients of 0.5 and 0.7. It can be seen however, that there is an over-prediction of power at the lower disc loading coefficient of 0.3 which implies a lack of separation prediction by the CFD within the diffuser.

7. Conclusions

A computational fluid dynamic model has been developed for the analysis of the Vortec 7. Flow visualisation of the Vortec 7 shows good agreement with CFD predictions. The use of the CFD model for the analysis of variations to the Vortec 7 has allowed cost effective modifications to be made. Development of new diffuser geometries, with predicted increases in air power, has been achieved with the aid of the CFD model. Comparison of the CFD predictions with wind tunnel investigations show similar results to those predicted. Refinement of the CFD model grid has improved the prediction of flow separation over the diffuser and improved agreement with wind tunnel data.

References

- Foreman, K.M. and Gilbert, B.L. (1983), "Experiments with a diffuser-augmented model wind turbine", *J. Energy Resour. Technol. Trans. ASME*, **105**(3), 46-53.
- Foreman, K.M., Maciulaitis, A. and Gilbert, B.L. (1983), "Performance predictions and recent data for advanced

- DAWT models”, ASME Solar Energy Division, Grumman Aerospace Corp., Bethpage, New York, April.
- Gilbert, B.L., Oman, R.A. and Foreman, K.M. (1978), “Fluid dynamics of diffuser-augmented wind turbines”, *J. Energy*, **2**(6), 368-374.
- Lilley, G.M. and Rainbird, W.J. (1956), “A preliminary report on the design and performance of ducted windmills”, CoA Report No. 102, The College of Aeronautics, Cranfield, April.
- Nash, T.A. (1997), “Design & construction of the Vortec 7”, *NZ Wind Energy Association, First Annual Conference*, Wellington, June.
- Phillips, D.G., Flay, R.G.J. and Nash, T.A. (1999), “Aerodynamic analysis and monitoring of the Vortec 7 diffuser augmented wind turbine”, *IPENZ Trans.*, Auckland, New Zealand, November.
- Richards, P.J. and Hoxey, R.P. (1993), “Appropriate boundary conditions for computational wind engineering models using the $k-\varepsilon$ turbulence model”, *J. Wind Eng. Ind. Aerod.*, **46 & 47**, 145-153.